한국추진공학회 2005년도 춘계학술대회 논문집 pp.47~52 2005 KSPE Spring Conference

고체추진기기의 고장분포 기반의 균열전파 모델: 실험과의 비교

여재익*

Failure distribution based crack propagation in solid propellant container: Comparison with experiment

Jai-ick Yoh*

ABSTRACT

We present a simple idea to simulate dynamic fracture and fragmentation of a propulsion system exposed to an extreme condition, such as a fire. The system consists of energetic materials confined in a steel cylinder. The strain failure model of the confinement is a modified Johnson-Cook model with a statistical failure distribution. By using the size distribution data of the fragments from the thermal explosion tests, the failure strain distribution can be empirically obtained and then entered into the model. The simulated fracture and fragment sizes are compared with the experimental records.

초 록

이 논문은 열폭발 실험에서의 열적, 화학적, 기계적 행동의 결과에 대한 3차원 모델 결과를 나타낸다. 폭발이 관찰되기 전까지 제한된 고 폭발물은 시간당 1℃의 비율로 가열된다. 임의의 Lagrangian - Euler 코드를 사용하여 모델링된 가열, 점화 그리고, deflagration 단계는 구조적에서 동적인 hydro 시간단계까지 변하는 넓은 범위의 시간 영역에서 다루어 질수 있다. Johnson-Cook Failure Model (JCFM)에 실험적 고장분포를 더하여 폭발기기의 균열방향과 fragment의 크기를 예측할 수 있는 모델을 개발한다.

Key Words: Solid Propellants (고체추진제), Propulsion System Crack (추진기기의 균열), Johnson-Cook Failure Model (JC 고장 모델), HMX

1. Introduction

In the energetic materials community, there is an interest in using computer simulations to reduce the number of experiments for weapons design and safety evaluation. Models and numerical strategies are being developed for the heating of energetic materials until

* 서울대학교 기계항공공학부
연락저자, E-mail: jjyoh@snu.ac.kr

reaction (cookoff). Munitions exposed to a fire are of great concern. In this case, time scales for behaviour can range from days to microseconds. During the relatively slow heating phase, the response of an energetic materials system is paced by thermal diffusion and chemical decomposition, while the mechanical response is essentially a quasi-static process. As the decomposition reactions accelerate, heat is generated faster than it can diffuse. Product gases are formed and the resulting pressure rises accelerate the energetic and containment material response. The resulting thermal explosion can range in violence from a pressure rupture to a detonation.

A number of investigators have modelled slow cookoff experiments. Chidester *et al.* [1] calculated explosion times for HMX- and TATB-based explosives subjected to varying confinement and thermal environments. Tarver and Tran [2] improved thermal decomposition models for HMX-based plastic bonded explosives and attained reasonable predictions for ignition time using the thermal-chemical code, Chemical TOPAZ. These thermo-chemical models were expanded to include hydro effects, and the earlier models were evaluated against small-scale tests. It was recognized that the models required further development and needed to be benchmarked against well-instrumented cookoff experiments. More recent modelling efforts have focused on wall strain rates as a measure of cookoff violence.

In the modeling work of this study, the process of cookoff is not separated into two regimes. Instead, a single calculation is performed for the heating, ignition, and explosive phases of cookoff. Coupled thermal, mechanical, and chemical models are used during all of these stages to account for effects such as chemical decomposition, burning, thermal expansion, and the closing of gaps. It is seen that the modelling of thermal explosions requires computational tools and models that can handle a wide variety of physical processes and time scales.

We consider the explosive LX-10 which has an HMX base [3]. The LX-10 has a nominal composition of 95% HMX and 5% Viton by weight.

In this paper, we investigate the response of confined HMX-based materials in our Scaled Thermal Explosion Experiment (STEX). The focuss is placed on the simulating of fracture and fragmentation of the confinement material, namely AerMet 100 steel. Efforts are made to compare the measured fragment sizes of explosively driven steel pipe. A numerical approach involving variable mass-scaling allows the calculation of coupled thermo-chemical-mechanical results over the widely varying time scales associated with the heating and explosive processes.

2. Experiment

In order to provide a database to test models, the STEX is designed to quantify the violence of thermal explosions under carefully controlled conditions [4]. The cylindrical test, shown in Fig. 1, is designed to provide ignition in the central region of the cylinder. The confinement vessel consists of AerMet 100 with heavily reinforced end caps which confine the decomposition gases until the tube wall fails. A length to diameter ratio of 4:1 is used for which the ID is 4.49 cm and the interior length is 20.3 cm. The wall thickness 0.3 cm for LX-10, giving an approximate

confinement pressure of 200 MPa. Ullage (air space) was included to allow for expansion of the HE without bursting the vessel prior to ignition. The total ullage that is present in the vessel was 8.66% for LX-10.

A feedback control system is used to adjust three radiant heaters to control the wall temperature at location no. 1 of Fig. 1(b). The thermocouples at location nos. 2 and 3 on the end caps are controlled with separate control loops. The wall thermocouple temperature is increased at 1 C/h until explosion. The lower and upper thermocouples are maintained at 4 and 9 C, respectively, below the wall temperature to provide for ignition near a plane half way between the two end caps. A probe with 5 thermocouples is used to monitor the internal temperature of the HE (see Fig. 1(b)). Two hoop strain gauges were used to measure the radial expansion of the tube at the axial midplane

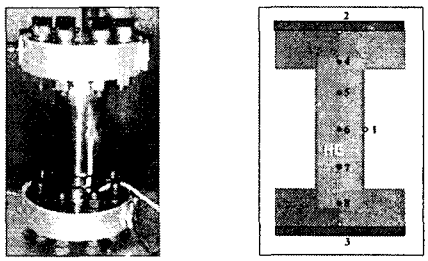

(a) (b)

Fig. 1 (a) Photograph of the STEX vessel. (b) Schematic of the model domain.

3. Models

3.1 Chemical model

The four-step, five-species reaction mechanism for HMX is

$$A \rightarrow B, r_1 = Z_1 \exp(-E_1/RT)\rho_A$$
$$B \rightarrow C, r_2 = Z_2 \exp(-E_2/RT)\rho_B$$
$$C \rightarrow D, r_3 = Z_3 \exp(-E_3/RT)\rho_C$$
$$D \rightarrow E, r_4 = Z_4 \exp(-E_4/RT)\rho_D^2$$

where A and B are solid species (β *and* δ phase HMX), C is solid intermediate, D and E are intermediate and final product gases, respectively. Here r_i is the mass reaction rate, Z_i is the frequency factor, and Ei is the activation energy for reaction *i*. Also ρ_j the mass concentration for species *j* = *A, B, C, D, E*.

The mechanism for Viton is a single-step, endothermic reaction:

$$Viton_{solid} \rightarrow Viton_{gas}, r_1 = Z_1 \exp(-E_1/RT)\rho_{Viton-solid}$$

The rate parameters in the above mechanisms for LX-10 are adjusted to fit One-Dimensional-Time-to-Explosion (ODTX) measurements. The values are given in [5].

After the chemical reactions have progressed significantly into the faster regime of cookoff in which changes are occurring on the time scale of the sound speed, a switch is made to a burn front model in which reactants are converted completely to products in a single reaction step. The burn front velocity, V is assumed to be a pressure-dependent function, and it takes the form $V = aP^n$, where V is in mm/s and P is in MPa.

This change in models is made for several reasons. First the Arrhenius models described above may not apply at the elevated temperatures and pressures of the burn process. The burn rate model is more useful since it can employ measured burn rates as described below. Finally, the computational effort required for the Arrhenius model is prohibitively large as a result of the fine mesh spacing and small time steps required to

model the narrow burn front. In contrast, solutions for the burn rate model can be obtained with practical amounts of computation time.

3.2 Thermal model

The time-dependent thermal transport model includes the effects of conduction, reaction, convection, and compression. The constant-volume heat capacity is constant for each reactant. The thermal conductivities of the solid species A, B and C are taken to be constant, whereas the effects of temperature are included for the gaseous species. The thermal properties for materials A, B and C are reported in [5] and use available measured values for LX-10. The heat capacity, cv, for gases D and E is assigned the same constant-volume value used in the gamma-law model. The temperature-dependent thermal conductivity is estimated at 1 kbar and T = 2000 C using Bridgmann's equation [6] for liquids in which the sound velocity is calculated using results from Cheetah [7].

As for the mechanical model, the discussion is quite involved and the readers are referred to the Refs. [8,9].

3.3 A modified Johnson-Cook Failure Model for AerMet 100

Simulations of an explosively-driven, steel cylinder were performed using the Johnson-Cook Failure Strain (JCFS) Model. The effects of the heterrogeneous microstructure were considered by incorporating Gaussian (spatial) distributions of the JCFS parameters (D_1 in Eqn. 2). The parameters used in the model are listed in Table 1. Fragmenting material motion was considered to be Lagrangian throughout the simulation. The idea is that the failure strain could not be constant in a material, else it would failure simultaneously over a dynamically loaded body with infinitesimally small fragments [11].

$$D = \sum \frac{\triangle \epsilon}{\triangle \epsilon_f} \tag{1}$$

$$\epsilon_f = D_1 + D_2 \exp D_3 \frac{-P}{\sigma_v} \tag{2}$$

4. Results

One-dimensional results are not discussed here and the readers are referred to Ref. [5,8,9,10]. Two dimensional simulations are performed for the STEX system LX-10. This system is assumed to be axisymmetric, and a cylindrical wedge was selected for the calculation domain. In Fig. 2, calculated temperatures of the STEX system are plotted versus time, along with measured curves. The measured and calculated temperatures are shown at an internal location (no. 6 in Fig. 1(b)) and the control location (no. 1 in Fig. 1(b)). The predicted and measured internal temperature curves are in good agreement for LX-10, and the predicted explosion temperature (TC no. 1) of 182 C agrees very well with the experimental value of 181.5 C.

Studies were conducted to assess the accuracy of the calculations and the reproducibility of the measurements. The model simulations were repeated with the refined meshes and are numerically accurate to less than a degree. Thus, the model results are numerically accurate and the measurements seem to be reproducible.

In Figs. 3, calculated vessel wall hoop strain for the STEX system is shown with the measurement over the duration of the tests.

The results confirm the accuracy of the hoop strain measurements and the Gruneisen EOS for AerMet 100. Near the ignition point, decomposition gases pressurize the vessel, and measured strains are greater than the empty-vessel results.

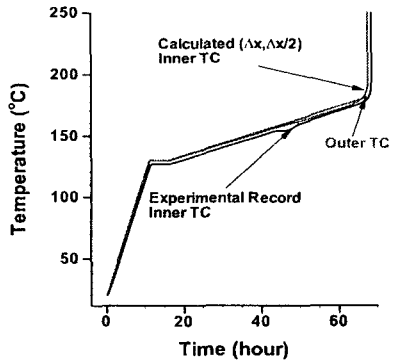

Fig. 2 Prediction of thermal response of confined LX-10.

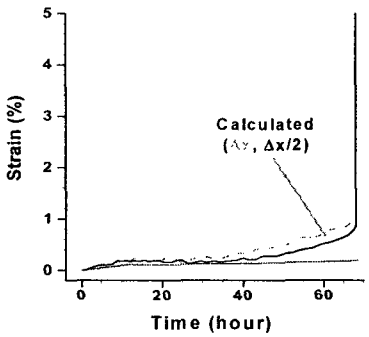

Fig. 3 Experimental and calculated hoop strain records from the slow heating to the thermal runaway phase for LX-10.

Fig. 4 Retrieved fragments from explosively driven AerMet 100 pipe.

Figure 4 shows retrieved fragements from the

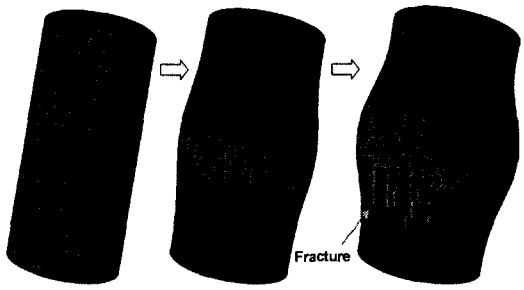

Fig. 5 Crack initiation on outer layer of the pipe under center loaded deflagration of HMX

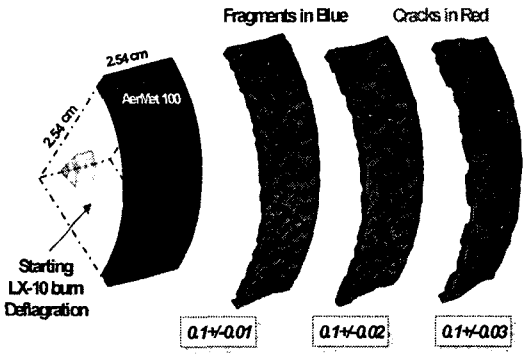

Fig. 6 Variation of *D1* parameter affecting the fragment size of metal pipe

actual STEX run of LX-10. The size distribution varies on the orders of several centimeters. Figure 5 shows three-dimensional numerical simulation of the same system. A distinct fracture pattern is observed and also the size of the unfailed zones (i.e. fragments) are on the order of 1-2 centimeters.

To understand the mechanism of present JCFM, we modified and varied D_1 parameter. The percent deviation of an assumed Gaussian distribution of the parameter is varied from 10, 20, and 30% as shown in Fig. 6. As the width of the bell-shaped distribution increases, the size of the crack (in red) in the simulation increases also. The unfailed zones which we identify as fragments are larger, and their presence is less frequent with increasing

distribution width.

Table 1. Parameters used in the fracture model

	Johnson-Cook Failure Coefficients for AerMet 100 Steel
D_1	0.1 +/- 20% standard deviation*
D_2	0.156**
D_3	0.296**

*Springer, Becker, Couch, 2003, **Chhabildas *et al.* 2001

5. Conclusions

A numerical investigation was performed to validate the experimental results for the thermally-induced explosion of the HMX-based explosive, LX-10. A particular interest is placed on the modeling of fracture and fragmentation of the AerMet 100 containment of LX-10, upon thermal explosion. A continued effort is needed to build a tool that can confidently address the fragmentation and also the violence of a thermal explosion system.

6. References

1. Chidester, S. K., Tarver, C. M., Green, L. G., and Urtiew, P. A., "On the Violence of Thermal Explosion in Solid Explosives," Combustion and Flame, 110, pp. 264-280, 1997.
2. Tarver, C. M., and Tran, T. D., Thermal Decomposition Models for HMX-based Plastic Bonded Explosives, Combustion and Flame, 137, pp50-62, 2004.
3. Meyer, R., Kohler, J., and Homburg, A, Explosives, Wiley-VCH, New York, 1993.
4. Wardell, J. F., and Maienschein, J. L., The Scaled Thermal Explosion Experiment, in Proceedings of 12th International Detonation Symposium, San Diego, CA, Office of Naval Research, 2002.
5. Yoh, J. J., McClelland, M. A., Nichols, A. L., Maienschein, J. L., and Tarver, C. M., Simulating Thermal Explosion of HMX-based Explosives: Model Comparison with Experiment, Lawrence Livermore National Laboratory, Technical Report, LLNL-JRNL-210733
6. Holman, J. P., Heat Transfer, McGraw-Hill, 1976, pp. 253-254.
7. Fried, L. E., and Howard, W. M., Cheetah 3.0 Users Manual, Lawrence Livermore National Laboratory, Livermore, CA, UCRL-MA-117541, 2001
8. Yoh, J. J., McClelland, M. A., Maienschein, J. L. Wardell, J. F., and Tarver, C. M., Simulating Thermal Explosion of RDX-based Explosives: Model Comparison with Experiment, Journal of Applied Physics, 97, 8, 2005
9. Yoh, J. J. McClelland, M. A. Maienschein, and J. L. Wardell, "Towards a Predictive Thermal Explosion Model for Energetic Materials," Journal of Computer-Aided Materials Design, 10, pp. 175-189, 2005.
10. 여재익, "화약 및 폭발성 물질의 열 반응 예측," 한국항공우주학회 춘계학술발표 논문집, 2005, pp.521-524
11. Mott, N. F., Proc. Roy. Soc. London, Series A, 189, pp. 300-308, 1947